

计算视觉与模式识别

光源

1 2 3 4 5 6 7 8 9 10 11 12 13 14 15 16 17 18 19 20 21 22 23 24 25 26 27 28 29 30 31 32 33 34 35 36 37

出射度

$$E(\mathbf{x}) = \int_{\Omega} L_e(\mathbf{x}, \theta_o, \varphi_o) \cos\theta(o) d\omega$$

定性辐射学

1 2 3 4 5 6 7 8 9 10 11 12 13 14 15 16 17 18 19 20 21 22 23 24 25 26 27 28 29 30 31 32 33 34 35 36 37

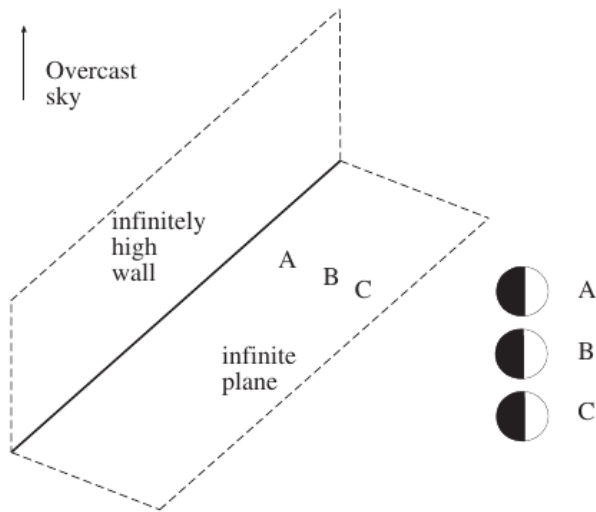


Figure 3.1. A geometry in which a qualitative radiometric solutions can be obtained by thinking about what the world looks like from the point of view of a patch. We wish to know what the brightness looks like at the base of two different infinitely high walls. In this geometry, an infinitely high matte black wall cuts off the view of the overcast sky — which is a hemisphere of infinite radius and uniform “brightness”. On the right, we show a representation of the directions that see or do not see the source at the corresponding points, obtained by flattening the hemisphere to a circle of directions (or, equivalently, by viewing it from above). Since each point has the same input hemisphere, the brightness must be uniform.

1 2 3 4 5 6 7 8 9 10 11 12 13 14 15 16 17 18 19 20 21 22 23 24 25 26 27 28 29 30 31 32 33 34 35 36 37

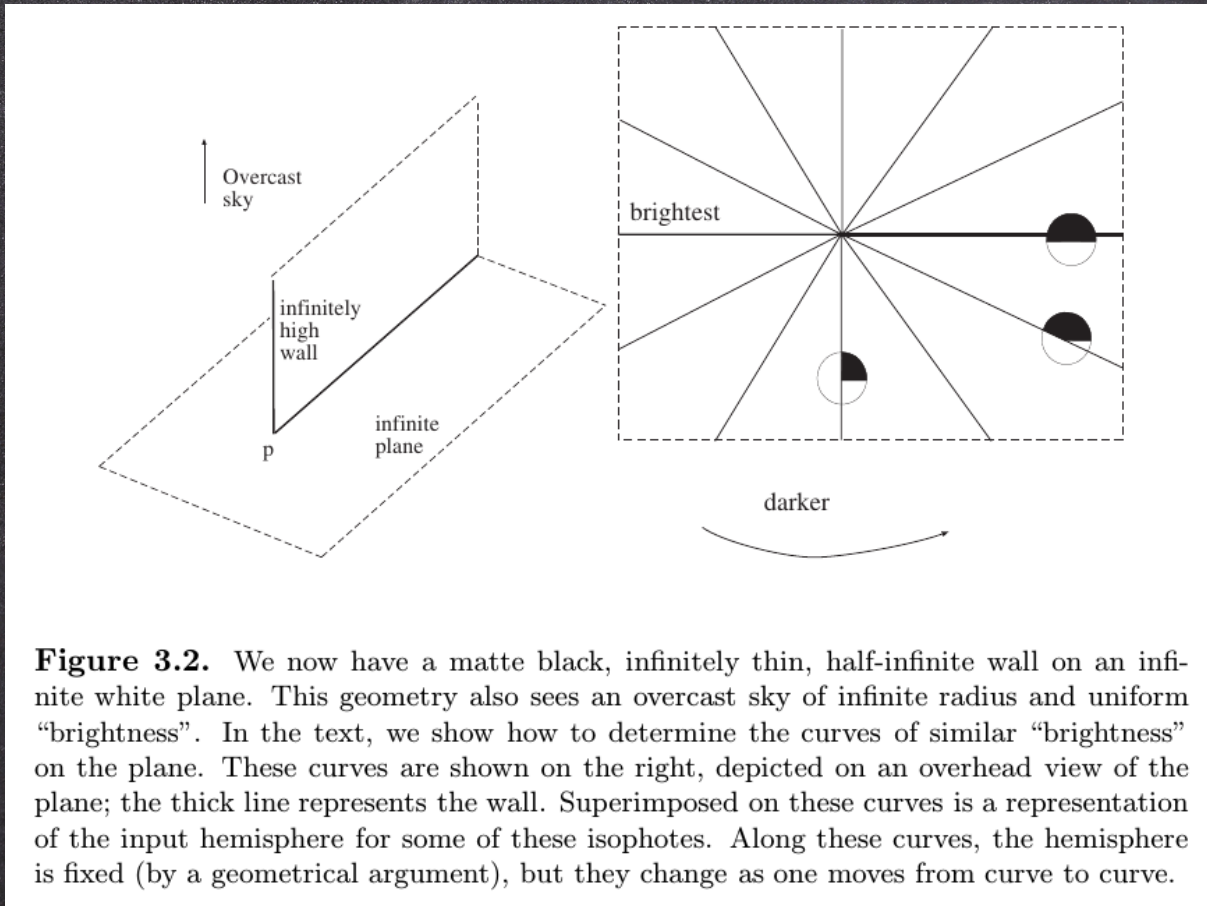


Figure 3.2. We now have a matte black, infinitely thin, half-infinite wall on an infinite white plane. This geometry also sees an overcast sky of infinite radius and uniform “brightness”. In the text, we show how to determine the curves of similar “brightness” on the plane. These curves are shown on the right, depicted on an overhead view of the plane; the thick line represents the wall. Superimposed on these curves is a representation of the input hemisphere for some of these isophotes. Along these curves, the hemisphere is fixed (by a geometrical argument), but they change as one moves from curve to curve.

光源效果

5/37

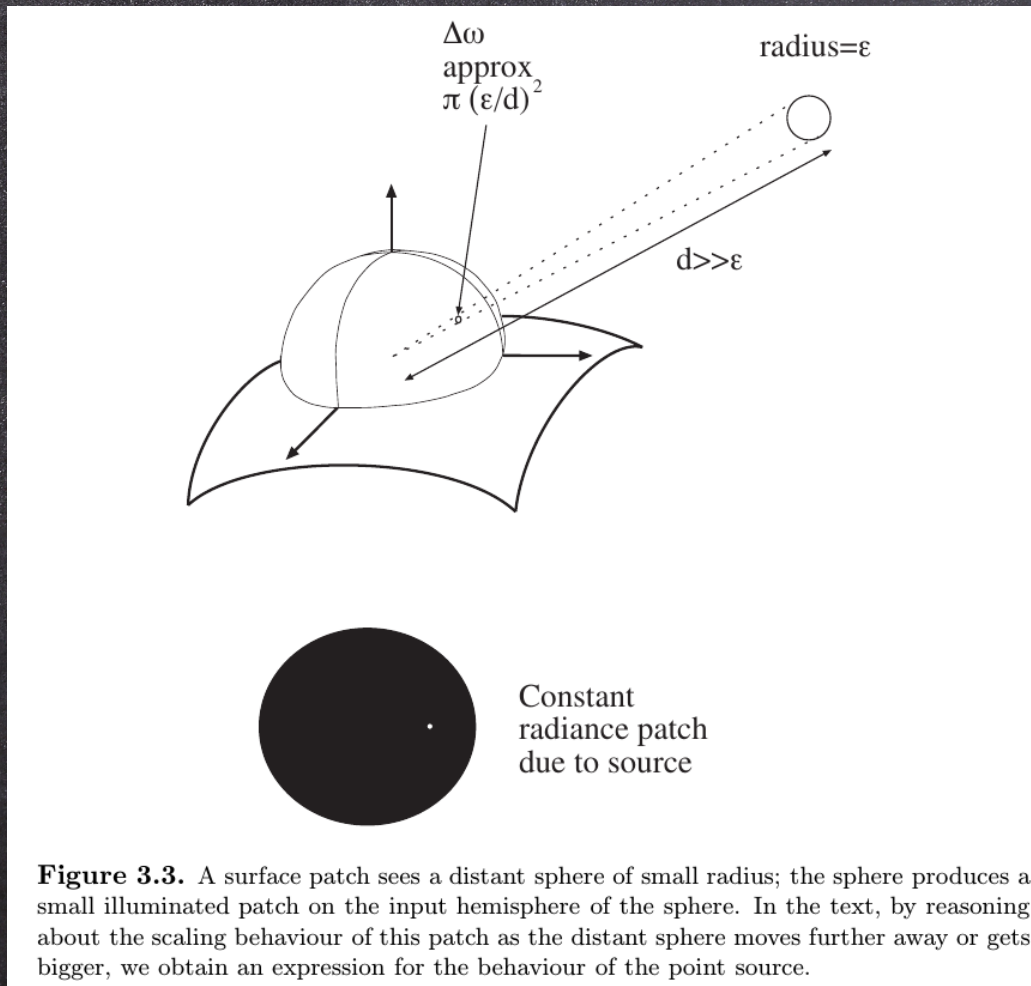


Figure 3.3. A surface patch sees a distant sphere of small radius; the sphere produces a small illuminated patch on the input hemisphere of the sphere. In the text, by reasoning about the scaling behaviour of this patch as the distant sphere moves further away or gets bigger, we obtain an expression for the behaviour of the point source.

1 2 3 4 5 6 7 8 9 10 11 12 13 14 15 16 17 18 19 20 21 22 23 24 25 26 27 28 29 30 31 32 33 34 35 36 37

发射度

$$E(x) = \int_{\Omega} L_e(x, \theta_o, \varphi_o) \cos \theta_o d\omega$$

辐射度

$$r \left(\frac{\varepsilon}{r} \right)^2 E \cos \theta$$

点光源

1 2 3 4 5 6 7 8 9 10 11 12 13 14 15 16 17 18 19 20 21 22 23 24 25 26 27 28 29 30 31 32 33 34 35 36 37

近点光源

$$\rho_d(\mathbf{x}) \frac{\mathbf{N}(\mathbf{x}) \cdot \mathbf{S}(\mathbf{x})}{r(\mathbf{x})^2}$$

无穷远点光源

$$\begin{aligned}\frac{\mathbf{N} \cdot \mathbf{S}(\mathbf{x})}{r(\mathbf{x})^2} &= \frac{\mathbf{N} \cdot (\mathbf{S}_0 + \Delta \mathbf{S}(\mathbf{x}))}{(r_0 + r(\mathbf{x}))^2} \\ &\approx \frac{\mathbf{N} \cdot \mathbf{S}_0}{r_0^2} \\ B(\mathbf{x}) &= \rho_d(\mathbf{x})(\mathbf{N} \cdot \mathbf{S})\end{aligned}$$

线光源

8/37

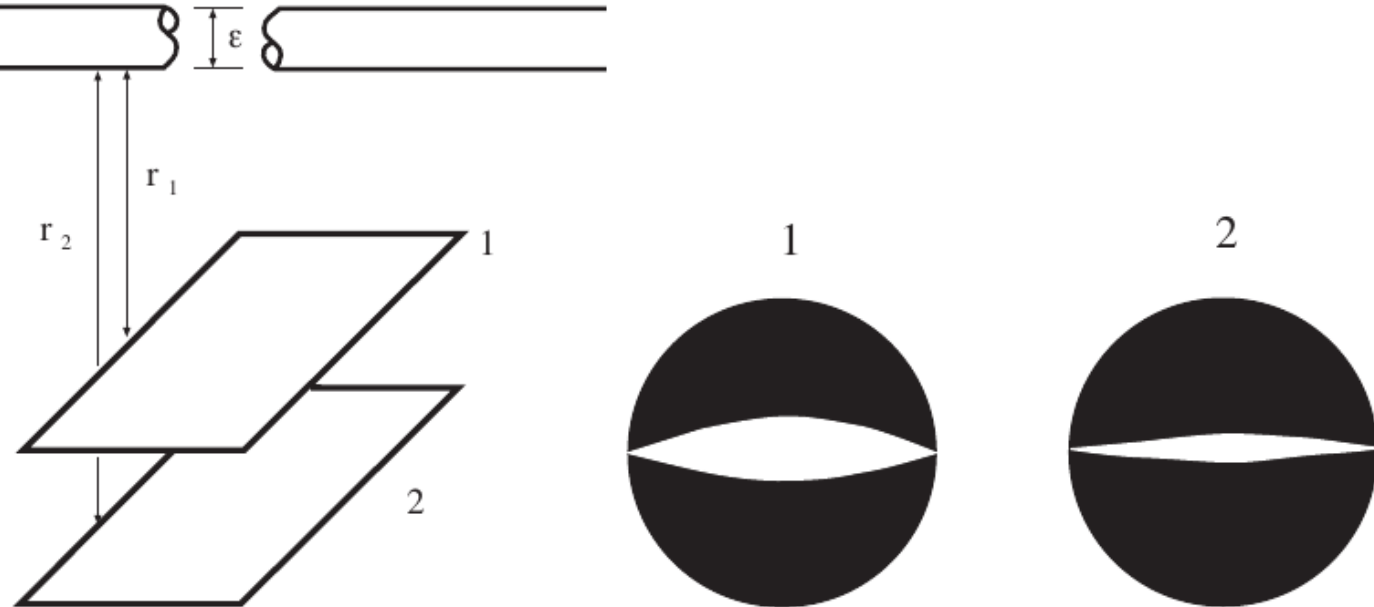


Figure 3.4. The radiosity due to a line source goes down as the reciprocal of distance, for points that are reasonably close to the source. On the left, two patches viewing an infinitely long, narrow cylinder with constant exitance along its surface and diameter ϵ . On the right, the view of the source *from each patch*, drawn as the underside of the input hemisphere seen from below. Notice that the length of the source on this hemisphere does not change, but the width does (as ϵ/r). This yields the result.

面光源

9/37

1 2 3 4 5 6 7 8 9 10 11 12 13 14 15 16 17 18 19 20 21 22 23 24 25 26 27 28 29 30 31 32 33 34 35 36 37

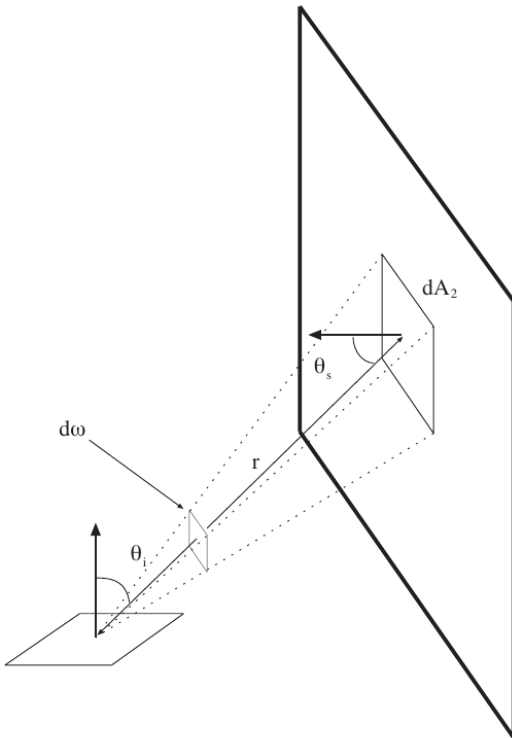


Figure 3.5. A diffuse source illuminates a diffuse surface. The source has exitance $E(\mathbf{u})$ and we wish to compute the radiosity on the patch due to the source. We do this by transforming the integral of incoming radiance at the surface into an integral over the source area. This transformation is convenient, because it avoids us having to use different angular domains for different surfaces; however, it still leads to an integral that is usually impossible in closed form.

面光源辐射度

1 2 3 4 5 6 7 8 9 10 11 12 13 14 15 16 17 18 19 20 21 22 23 24 25 26 27 28 29 30 31 32 33 34 35 36 37

$$\begin{aligned}
 B(\mathbf{x}) &= \rho_d(\mathbf{x}) \int_{\Omega} L_i(\mathbf{x}, \mathbf{u} \rightarrow \mathbf{x}) \cos\theta_i d\omega \\
 &= \rho_d(\mathbf{x}) \int_{\Omega} L_e(\mathbf{u}, \mathbf{u} \rightarrow \mathbf{x}) \cos\theta_i d\omega \\
 &= \rho_d(\mathbf{x}) \int_{\Omega} \left(\frac{E(\mathbf{u})}{\pi} \right) \cos\theta_i d\omega \\
 &= \rho_d(\mathbf{x}) \int_{\text{Source}} \left(\frac{E(\mathbf{u})}{\pi} \right) \cos\theta_i \left(\cos\theta_s \frac{dA_{\mathbf{u}}}{r^2} \right) \\
 &= \rho_d(\mathbf{x}) \int_{\text{Source}} \frac{E(\mathbf{u}) \cos\theta_i \cos\theta_s}{\pi r^2} dA_{\mathbf{u}}
 \end{aligned}$$

- $E(\mathbf{u}) = \pi L_e(\mathbf{u}, \mathbf{u} \rightarrow \mathbf{x})$

局部光照模型——点光源

1 2 3 4 5 6 7 8 9 10 11 12 13 14 15 16 17 18 19 20 21 22 23 24 25 26 27 28 29 30 31 32 33 34 35 36 37

点光源

$$B(\mathbf{x}) = \sum_{s \in \{t | t \rightarrow x\}} B_s(\mathbf{x})$$

无穷远点光源

$$B(\mathbf{x}) = \sum_{s \in \{t | t \rightarrow x\}} \rho_d(\mathbf{x}) \mathbf{N}(\mathbf{x}) \cdot \mathbf{S}_s$$

近点光源

$$B(\mathbf{x}) = \sum_{s \in \{t | t \rightarrow x\}} \rho_d(\mathbf{x}) \frac{\mathbf{N}(\mathbf{x}) \cdot \mathbf{S}(\mathbf{x})}{r_s(\mathbf{x})^2}$$

点光源与阴影

12/37

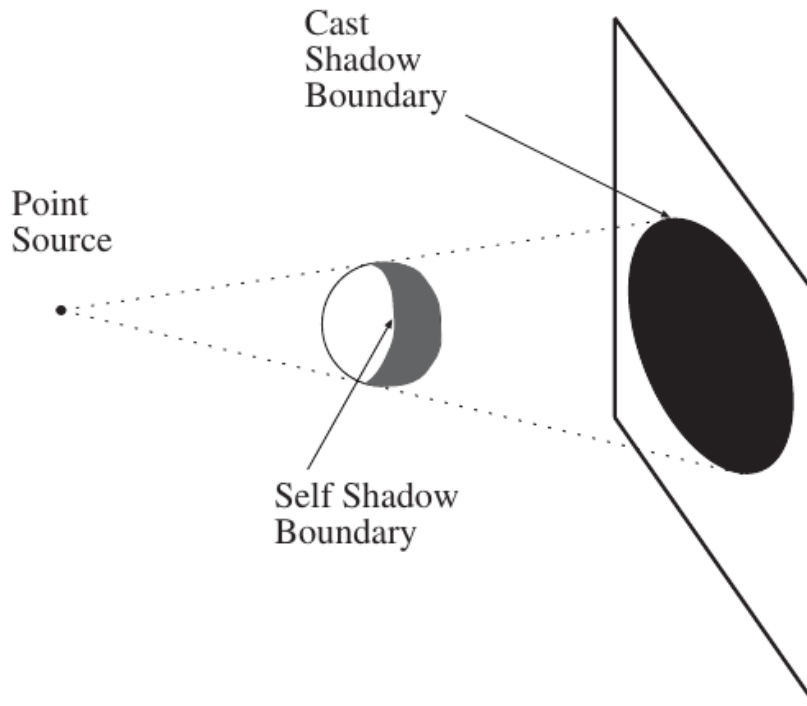


Figure 3.6. Shadows cast by point sources on planes are relatively simple. Self shadow boundaries occur when the surface turns away from the light and cast shadow boundaries occur when a distant surface occludes the view of the source.

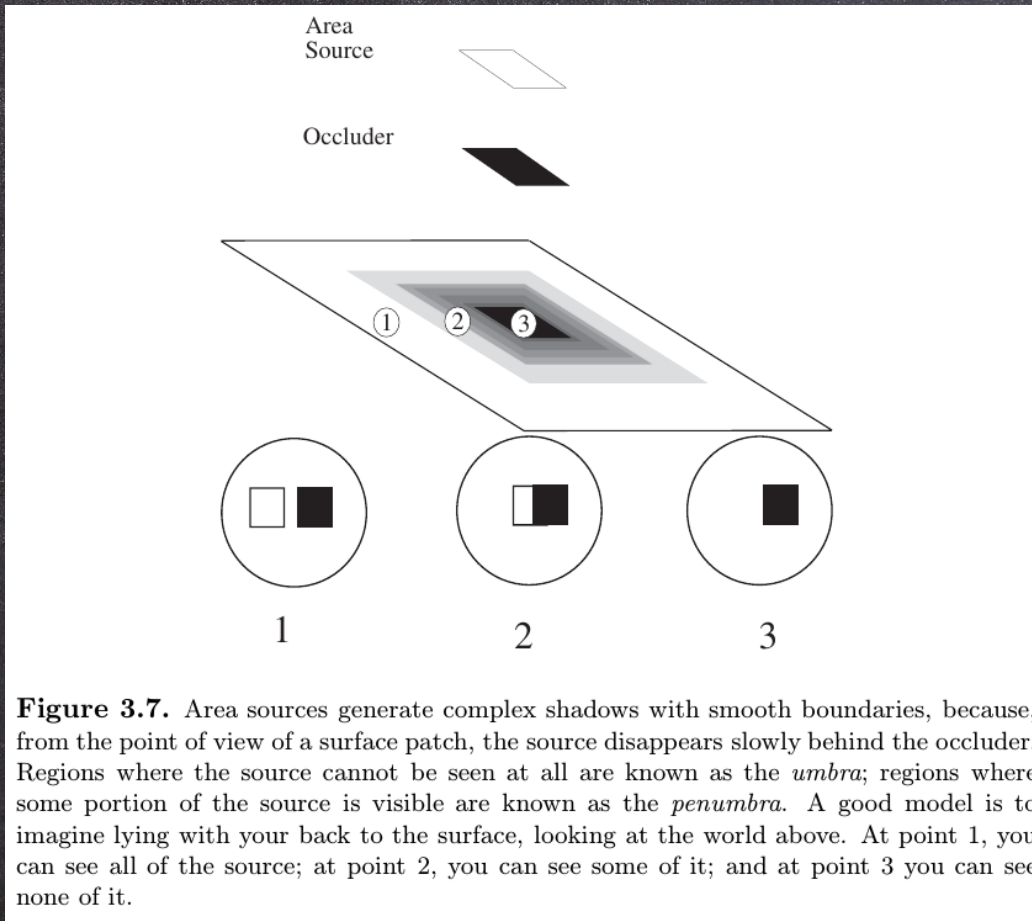
面光源

1 2 3 4 5 6 7 8 9 10 11 12 13 14 15 16 17 18 19 20 21 22 23 24 25 26 27 28 29 30 31 32 33 34 35 36 37

$$\begin{aligned} B(\mathbf{x}) &= \sum_{s \in \text{all sources}} \left\{ \int_{\text{visible component of sources } s} \text{Radiosity due to source} \right\} \\ &= \sum_{s \in \text{all sources}} \int_{\text{visible component of sources } s} \left\{ E(\mathbf{u}) \frac{\cos\theta_u \cos\theta_s}{\pi r^2} dA_{\mathbf{u}} \right\} \end{aligned}$$

面光源与阴影

1 2 3 4 5 6 7 8 9 10 11 12 13 14 15 16 17 18 19 20 21 22 23 24 25 26 27 28 29 30 31 32 33 34 35 36 37



环境光

15/37

1 2 3 4 5 6 7 8 9 10 11 12 13 14 15 16 17 18 19 20 21 22 23 24 25 26 27 28 29 30 31 32 33 34 35 36 37

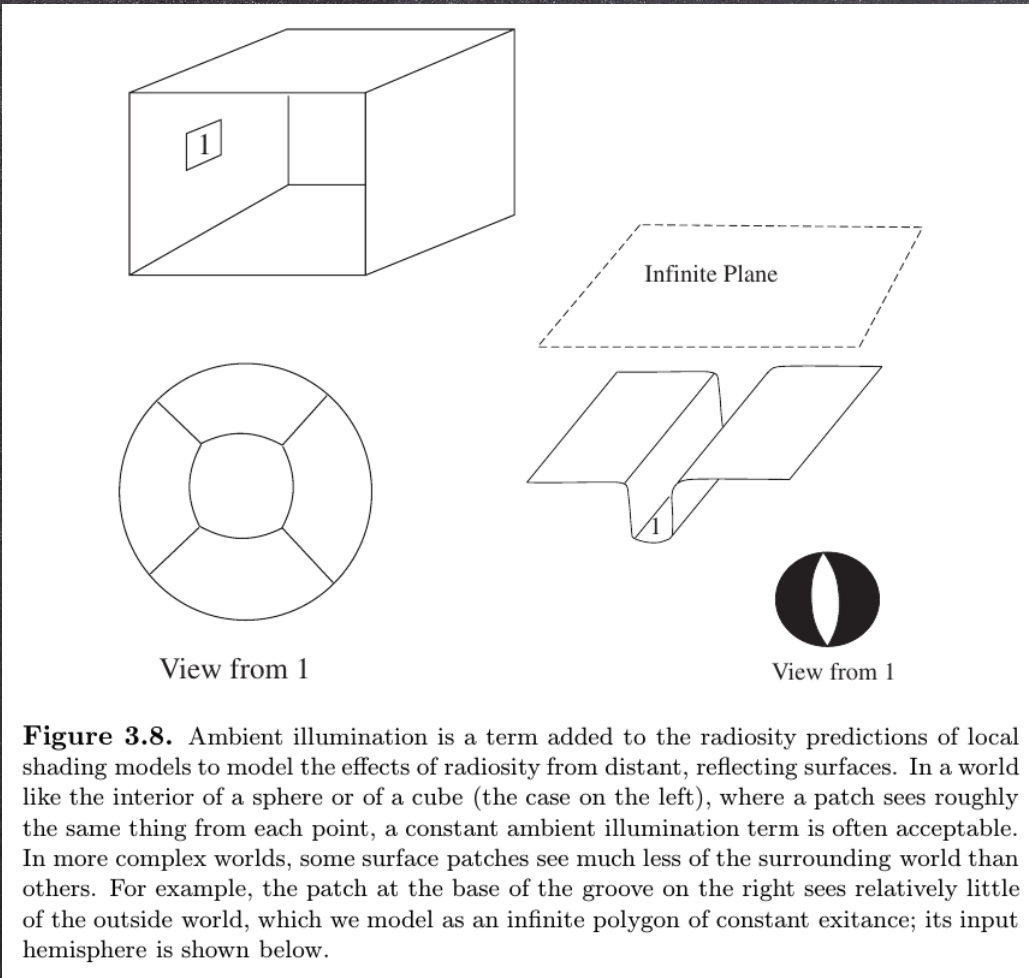
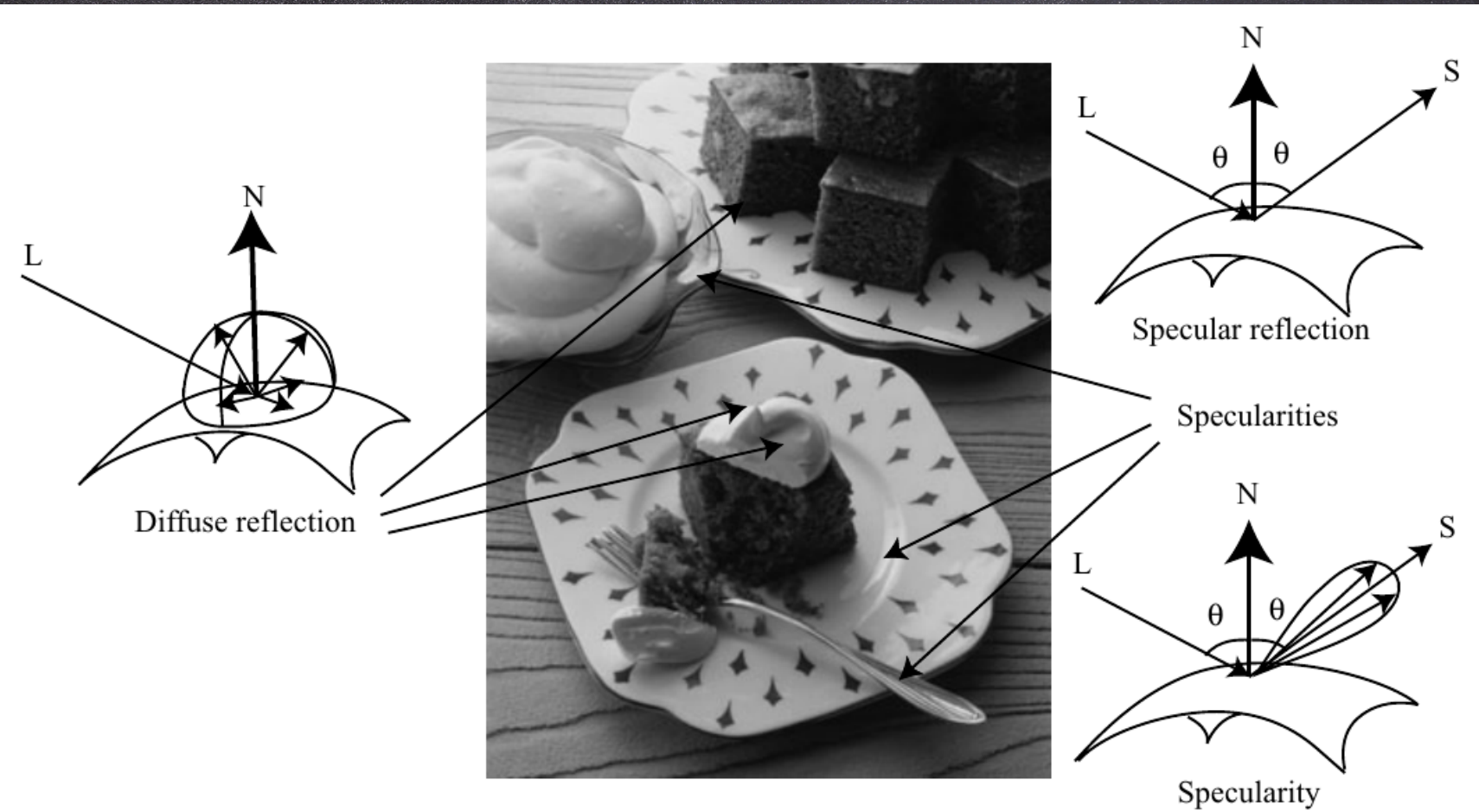


Figure 3.8. Ambient illumination is a term added to the radiosity predictions of local shading models to model the effects of radiosity from distant, reflecting surfaces. In a world like the interior of a sphere or of a cube (the case on the left), where a patch sees roughly the same thing from each point, a constant ambient illumination term is often acceptable. In more complex worlds, some surface patches see much less of the surrounding world than others. For example, the patch at the base of the groove on the right sees relatively little of the outside world, which we model as an infinite polygon of constant exitance; its input hemisphere is shown below.

表面反射

16/37

1 2 3 4 5 6 7 8 9 10 11 12 13 14 15 16 17 18 19 20 21 22 23 24 25 26 27 28 29 30 31 32 33 34 35 36 37



朗伯与镜面反射模型

1 2 3 4 5 6 7 8 9 10 11 12 13 14 15 16 17 18 19 20 21 22 23 24 25 26 27 28 29 30 31 32 33 34 35 36 37

$$\begin{array}{llll} I(\mathbf{x}) & = & \rho(\mathbf{x})(\mathbf{N} \cdot \mathbf{S}) \text{Vis}(\mathbf{S}, \mathbf{x}) & + \rho(\mathbf{x})A \\ \text{Image} & & \text{Diffuse} & + \text{Ambient} + \text{Specular(mirror-like)} \\ \text{intensity} & & \text{term} & \text{term} \end{array}$$

辐射标定

1 2 3 4 5 6 7 8 9 10 11 12 13 14 15 16 17 18 19 20 21 22 23 24 25 26 27 28 29 30 31 32 33 34 35 36 37

$$\begin{aligned} I_{ij}^{(k)} &= f(E_{ij}\Delta t_k) \\ \log g(I_{ij}^{(k)}) &= \log E_{ij} + \log \Delta t_k \end{aligned}$$

估计 $g = f^{-1}$, 损失函数:

$$\sum_{i,j,k} (\log g(I_{ij}^{(k)}) - (\log E_{ij} + \log \Delta t_k))^2 + \text{smoothness penalty on } g$$

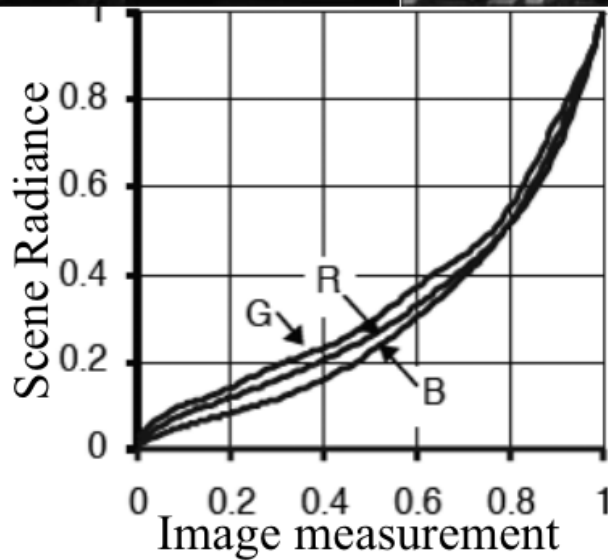
估计 E_{ij}

$$\sum_k w(I_{ij})(I_{ij}^{(k)} - f(E_{ij}\Delta t_k))^2$$

辐射标定示例

19/37

1 2 3 4 5 6 7 8 9 10 11 12 13 14 15 16 17 18 19 20 21 22 23 24 25 26 27 28 29 30 31 32 33 34 35 36 37



镜面反射形状

20/37

1 2 3 4 5 6 7 8 9 10 11 12 13 14 15 16 17 18 19 20 21 22 23 24 25 26 27 28 29 30 31 32 33 34 35 36 37

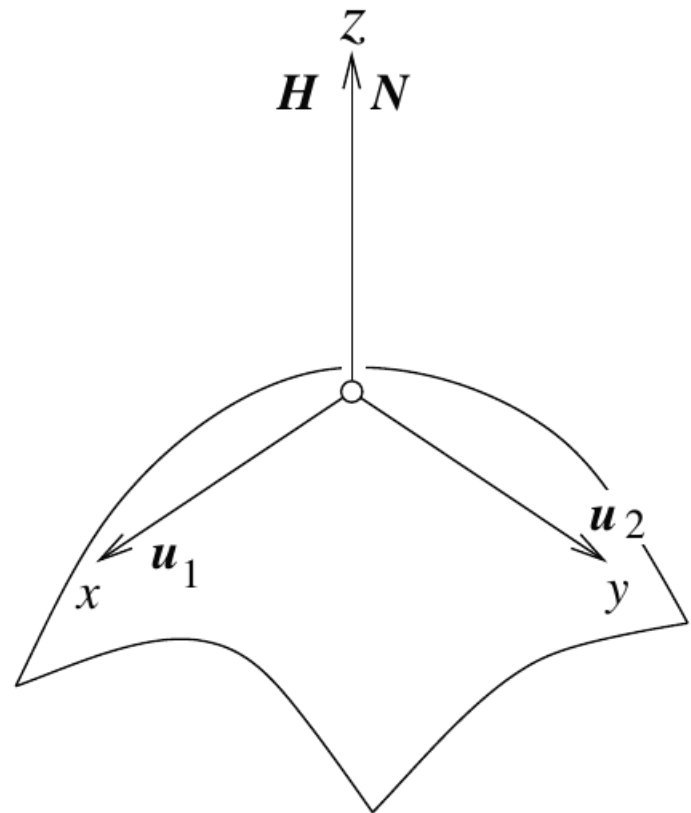
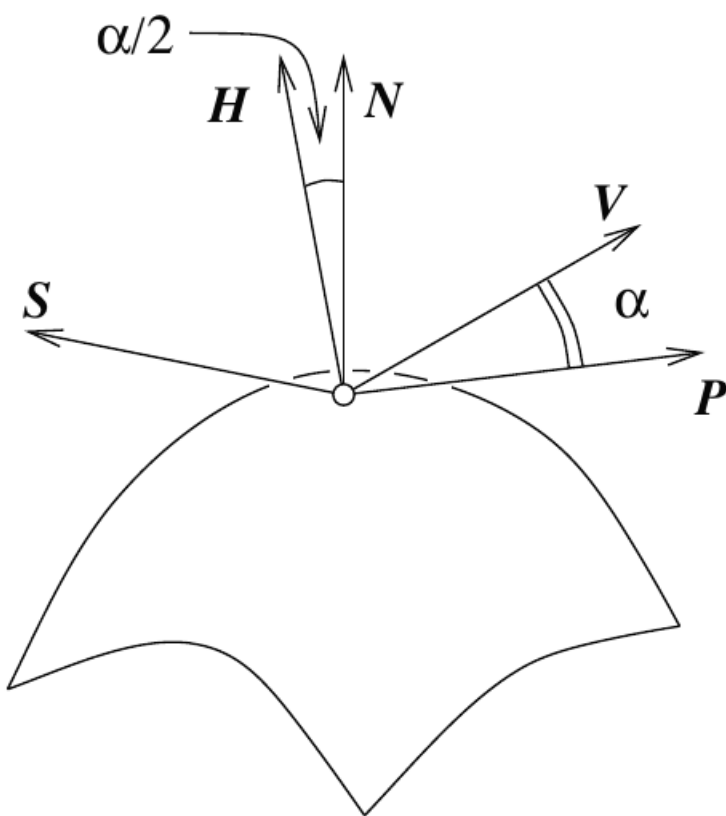


FIGURE 2.6: A specular surface viewed by a distant observer. We establish a coordinate system at the brightest point of the specularity (where the half-angle direction is equal to the normal) and orient the system using the normal and principal directions.

镜面反射的边界

1 2 3 4 5 6 7 8 9 10 11 12 13 14 15 16 17 18 19 20 21 22 23 24 25 26 27 28 29 30 31 32 33 34 35 36 37

$$\mathbf{V} \cdot \mathbf{P} \geq 1 - \varepsilon$$

$$\begin{aligned} 1 - \varepsilon &= \mathbf{V} \cdot \mathbf{P} \\ &= 2 \frac{(\mathbf{H} \cdot \mathbf{N})^2}{(\mathbf{H} \cdot \mathbf{H})} - 1 \end{aligned}$$

$$z = -\frac{1}{2}(\kappa_1 x^2 + \kappa_2 y^2)$$

$$\mathbf{N} = (1 + \kappa_1^2 x^2 + \kappa_2^2 y^2)^{-\frac{1}{2}} (\begin{matrix} \kappa_1 x & \kappa_2 y & 1 \end{matrix})^T$$

$$\kappa_1^2 x^2 + \kappa_2^2 y^2 = \zeta$$

镜面反射的移动

22/37

1 2 3 4 5 6 7 8 9 10 11 12 13 14 15 16 17 18 19 20 21 22 23 24 25 26 27 28 29 30 31 32 33 34 35 36 37

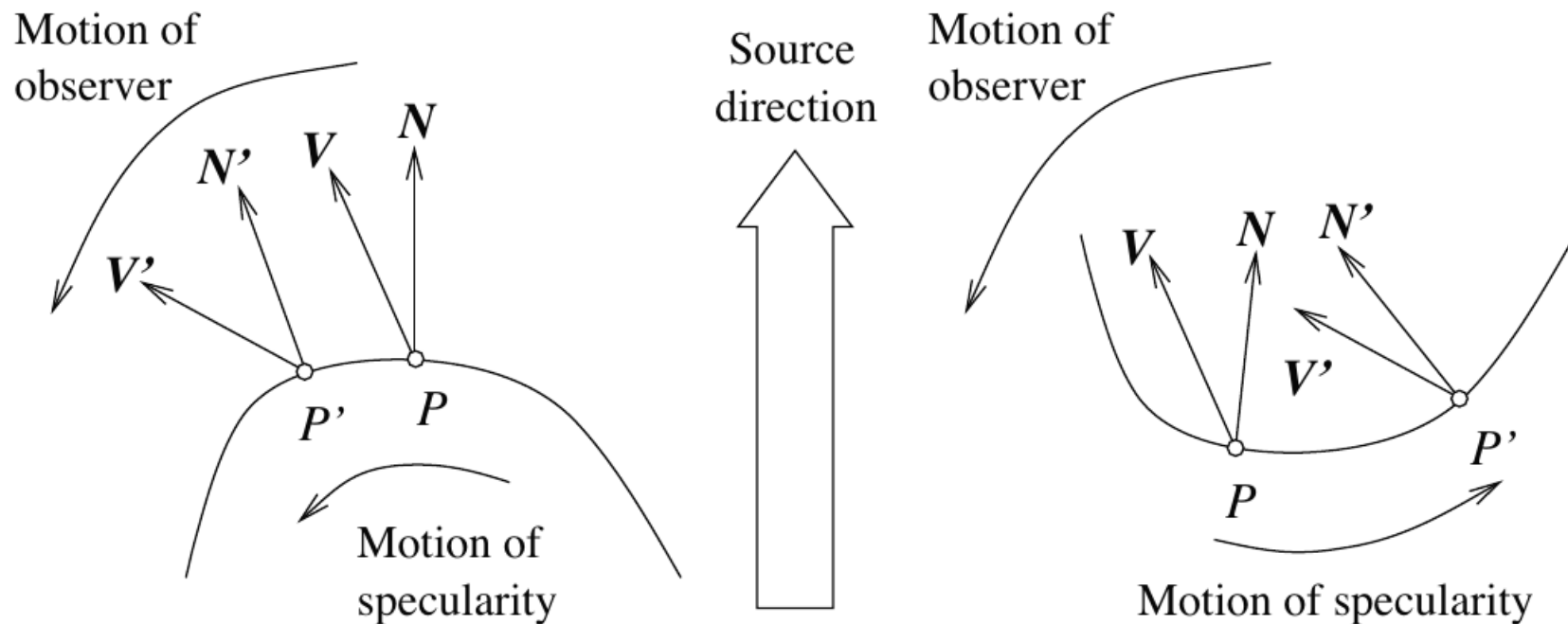


FIGURE 2.7: Specularities on convex and concave surfaces behave differently when the view changes. With an appropriate choice of source direction and motion, this could be used to obtain the signs of the principal curvatures.

1 2 3 4 5 6 7 8 9 10 11 12 13 14 15 16 17 18 19 20 21 22 23 24 25 26 27 28 29 30 31 32 33 34 35 36 37

\mathbf{S} 不变：

$$\begin{aligned}\mathbf{V} &= 2(\mathbf{S} \cdot \mathbf{N})\mathbf{N} - \mathbf{S} \\ \delta\mathbf{V} &= 2(\mathbf{S} \cdot (\mathbf{N} + \delta\mathbf{N}))(\mathbf{N} + \delta\mathbf{N}) - \mathbf{S} - \mathbf{V} \\ &= 2(\mathbf{S} \cdot \delta\mathbf{N})\mathbf{N} + 2(\mathbf{S} \cdot \mathbf{N})\delta\mathbf{N} + 2(\mathbf{S} \cdot d\mathbf{N})d\mathbf{N} \\ d\mathbf{V} &= 2(\mathbf{S} \cdot d\mathbf{N})\mathbf{N} + 2(\mathbf{S} \cdot \mathbf{N})d\mathbf{N} + 2(\mathbf{S} \cdot d\mathbf{N})d\mathbf{N}\end{aligned}$$

得

$$d\mathbf{V} \cdot d\mathbf{r} = 2(\mathbf{S} \cdot \mathbf{N})d\mathbf{N} \cdot d\mathbf{r} \quad d\mathbf{r} = \mathbf{r}_s ds$$

亮度与照度推理

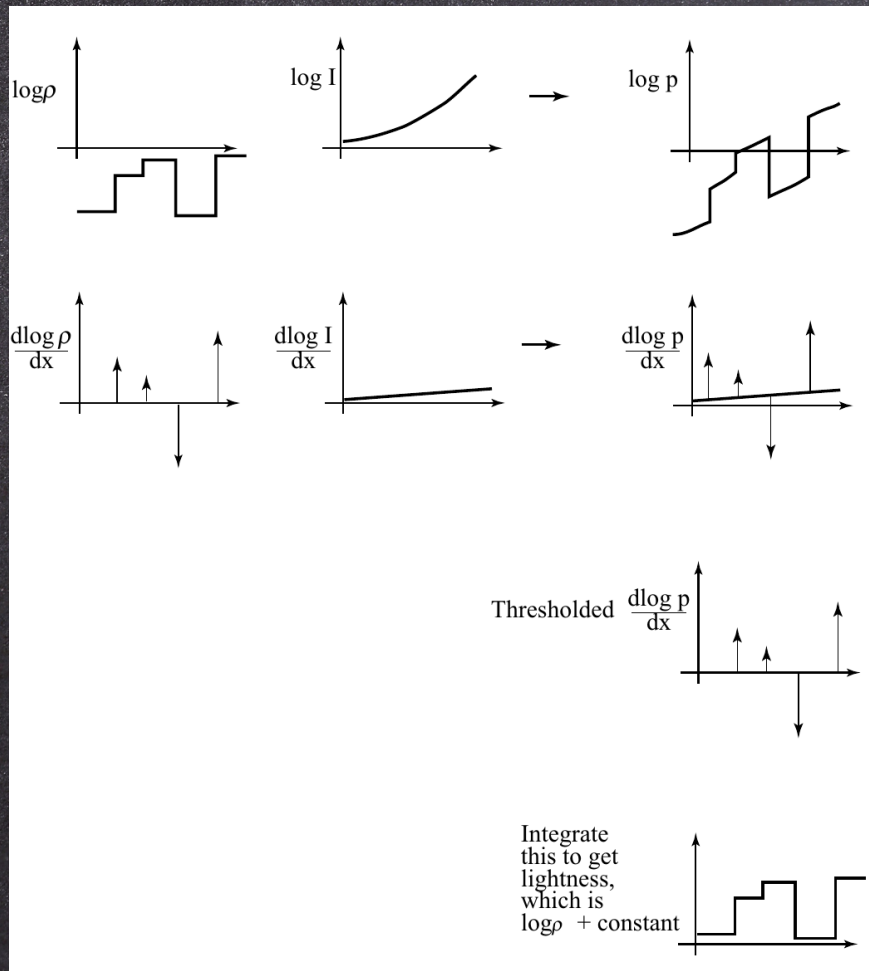
1 2 3 4 5 6 7 8 9 10 11 12 13 14 15 16 17 18 19 20 21 22 23 24 25 26 27 28 29 30 31 32 33 34 35 36 37

相机响应

$$\begin{aligned}C(\mathbf{x}) &= k_c I(\mathbf{x}) \rho(\mathbf{x}) \\ \log C(\mathbf{x}) &= \log k_c + \log I(\mathbf{x}) + \log \rho(\mathbf{x})\end{aligned}$$

- $\rho(\mathbf{x})$: 反射率
同一物体基本不变，不同物体边界处有突变
- $I(\mathbf{x})$: 光照
变化缓慢

亮度算法示例



估计反射率

1 2 3 4 5 6 7 8 9 10 11 12 13 14 15 16 17 18 19 20 21 22 23 24 25 26 27 28 29 30 31 32 33 34 35 36 37

- 计算阈值化梯度
- 积分

或

- 计算阈值化梯度 p, q
- 最小化

$$|\mathcal{M}_x l - p|^2 + |\mathcal{M}_y l - q|^2$$

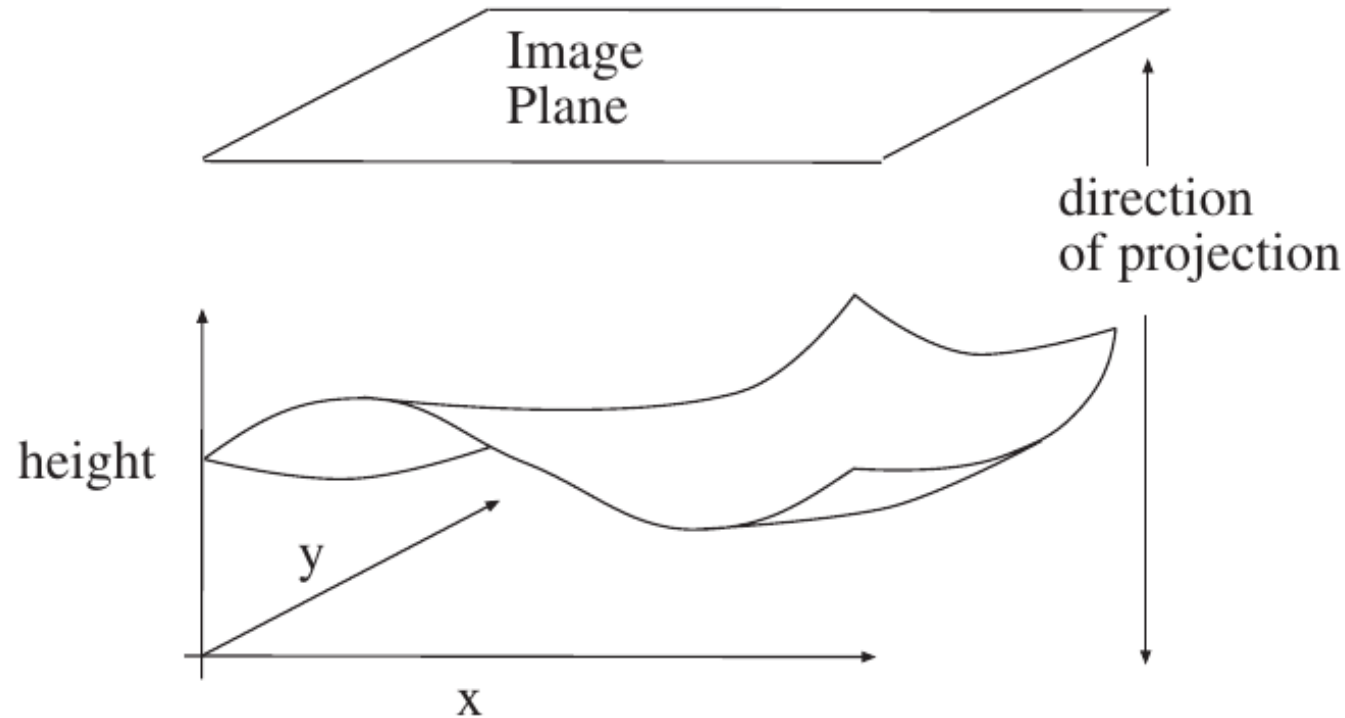


Figure 3.9. A Monge patch is a representation of a piece of surface as a height function. For the photometric stereo example, we assume that an orthographic camera — one that maps (x, y, z) in space to (x, y) in the camera — is viewing a Monge patch. This means that the shape of the surface can be represented as a function of position in the image.

1 2 3 4 5 6 7 8 9 10 11 12 13 14 15 16 17 18 19 20 21 22 23 24 25 26 27 28 29 30 31 32 33 34 35 36 37

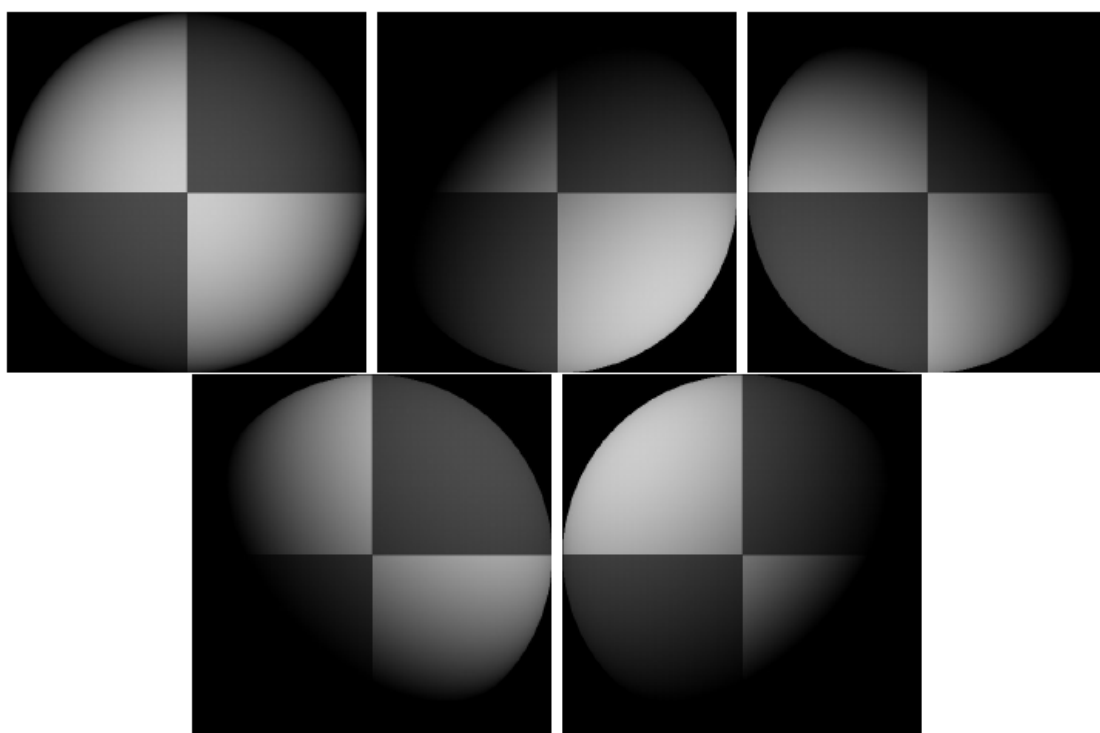


Figure 3.10. Five synthetic images of a sphere, all obtained in an orthographic view from the same viewing position. These images are shaded using a local shading model and a distant point source. This is a convex object, so the only view where there is no visible shadow occurs when the source direction is parallel to the viewing direction. The variations in brightness occurring under different sources code the shape of the surface.

图像与法向量

1 2 3 4 5 6 7 8 9 10 11 12 13 14 15 16 17 18 19 20 21 22 23 24 25 26 27 28 29 30 31 32 33 34 35 36 37

$$\begin{aligned}B(x) &= \rho(x) \mathbf{N}(x) \cdot \mathbf{S}_1 \\I(x, y) &= kB(\mathbf{x}) \\&= kB(x, y) \\&= k\rho(x, y) \mathbf{N}(x, y) \cdot \mathbf{S}_1 \\&= \mathbf{g}(x, y) \cdot \mathbf{V}_1 \\g(x, y) &= \rho(x, y) \mathbf{N}(x, y) \\V_1 &= k\mathbf{S}_1\end{aligned}$$

法向量计算

1 2 3 4 5 6 7 8 9 10 11 12 13 14 15 16 17 18 19 20 21 22 23 24 25 26 27 28 29 30 31 32 33 34 35 36 37

$$\begin{aligned}\mathbf{i}(x, y) &= (I_1(x, y) \ I_2(x, y) \ \cdots \ I_n(x, y))^T \\ &= \mathcal{V} \mathbf{g}(x, y) \\ \mathcal{V} &= \begin{pmatrix} \mathbf{V}_1^T \\ \mathbf{V}_2^T \\ \vdots \\ \mathbf{V}_n^T \end{pmatrix}\end{aligned}$$

得

$$\begin{aligned}\mathbf{N}(x, y) &= \frac{\mathbf{g}(x, y)}{|\mathbf{g}(x, y)|} \\ |\mathbf{g}(x, y)| &= \rho(x, y)\end{aligned}$$

法向量场

31/37

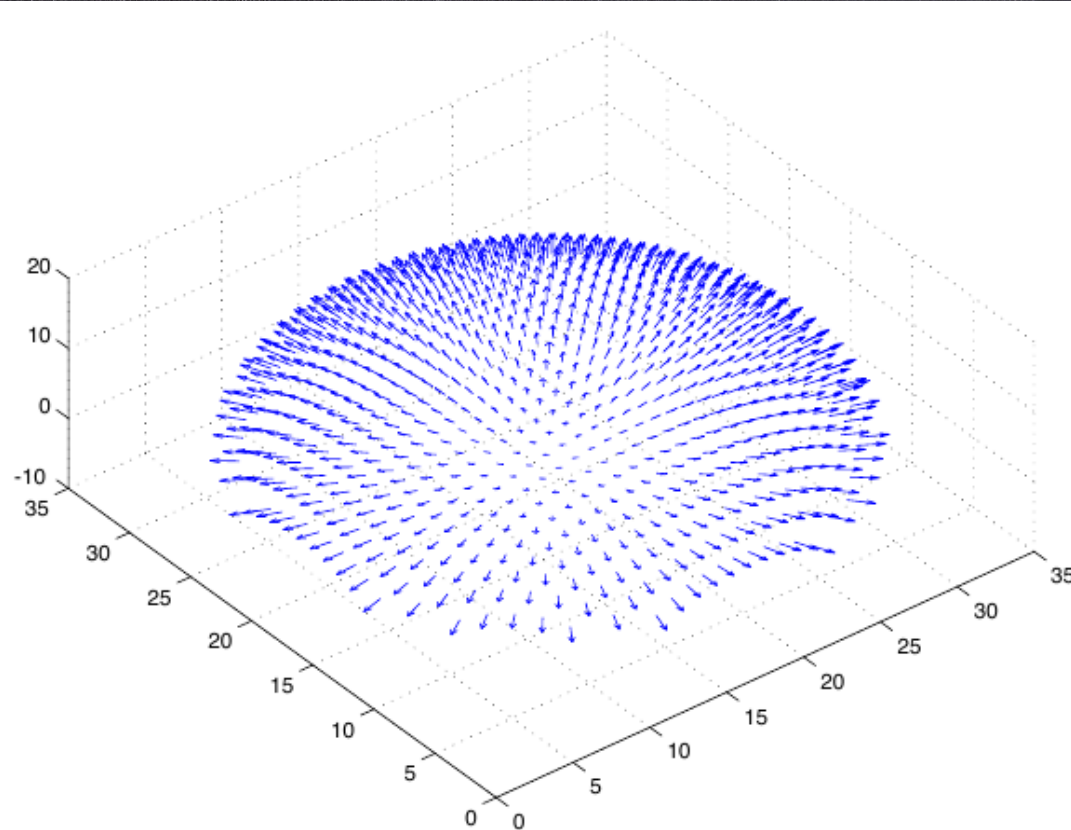


Figure 3.13. The normal field recovered from the surface of figure 3.10.

从法向量获取形状

1 2 3 4 5 6 7 8 9 10 11 12 13 14 15 16 17 18 19 20 21 22 23 24 25 26 27 28 29 30 31 32 33 34 35 36 37

$$\mathbf{N}(x, y) = \left(1 + \frac{\partial f^2}{\partial x} + \frac{\partial f^2}{\partial y} \right)^{-\frac{1}{2}} \begin{pmatrix} \frac{\partial f}{\partial x} & \frac{\partial f}{\partial y} & 1 \end{pmatrix}^T$$

$$f(x, y) = \oint_C \begin{pmatrix} \frac{\partial f}{\partial x} & \frac{\partial f}{\partial y} \end{pmatrix}^T \cdot d\mathbf{l} + c$$

$$l: (0, 0) \rightarrow (0, v) \rightarrow (u, v)$$

$$f(u, v) = \int_o^v \frac{\partial f}{\partial y} (0 \ y) dy + \int_o^u \frac{\partial f}{\partial x} (x \ v) dx + c$$

法向量场到高度场

33/37

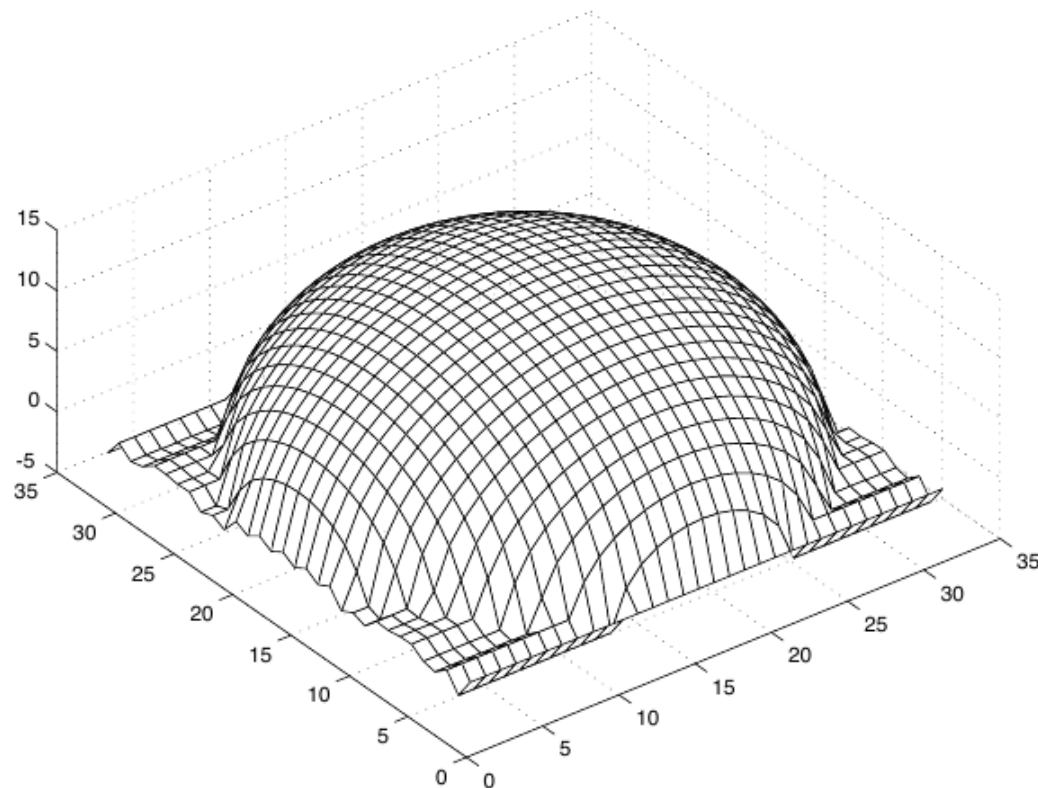


Figure 3.14. The height field obtained by integrating this normal field using the method described in the text.

互反射

1 2 3 4 5 6 7 8 9 10 11 12 13 14 15 16 17 18 19 20 21 22 23 24 25 26 27 28 29 30 31 32 33 34 35 36 37

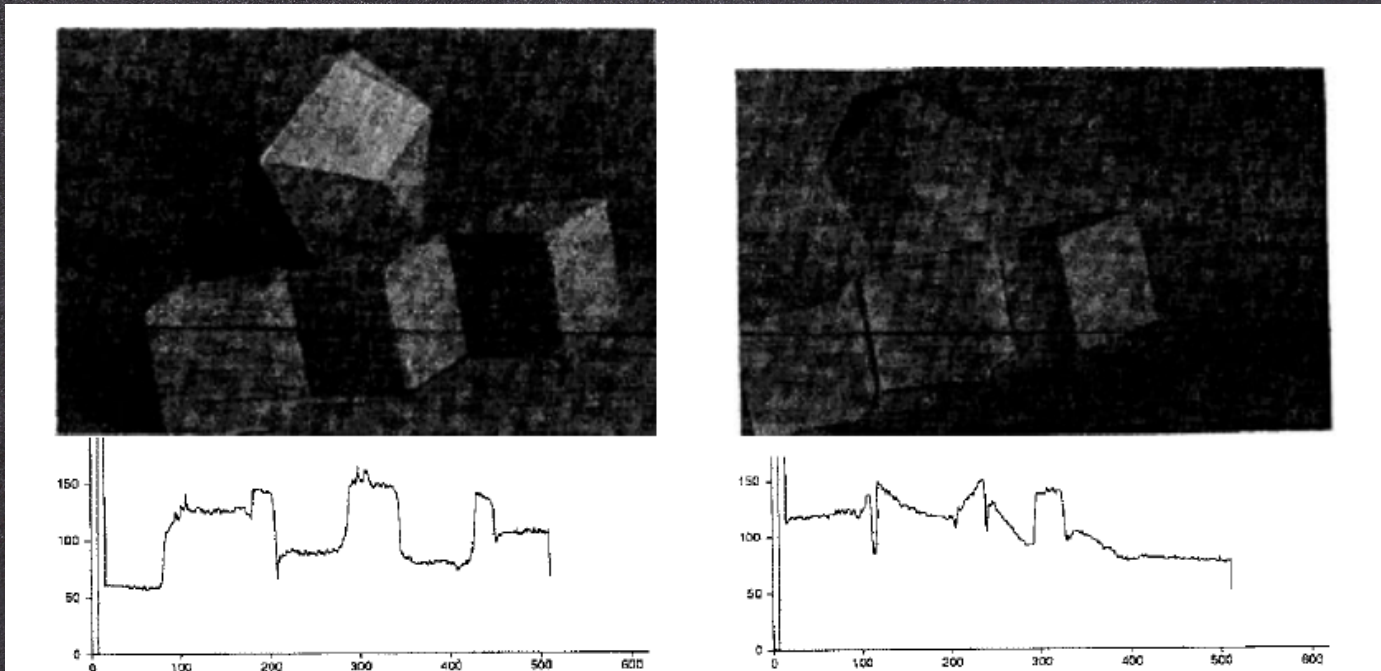


Figure 3.15. The column on the left shows data from a room with matte black walls and containing a collection of matte black polyhedral objects; that on the right shows data from a white room containing white objects. The images are qualitatively different, with darker shadows and crisper boundaries in the black room, and bright reflexes in the concave corners in the white room. The graphs show sections of the image intensity along the corresponding lines in the images. *Figure from “Mutual Illumination,” by D.A. Forsyth and A.P. Zisserman, Proc. CVPR, 1989, © 1989 IEEE*

互反射模型

1 2 3 4 5 6 7 8 9 10 11 12 13 14 15 16 17 18 19 20 21 22 23 24 25 26 27 28 29 30 31 32 33 34 35 36 37

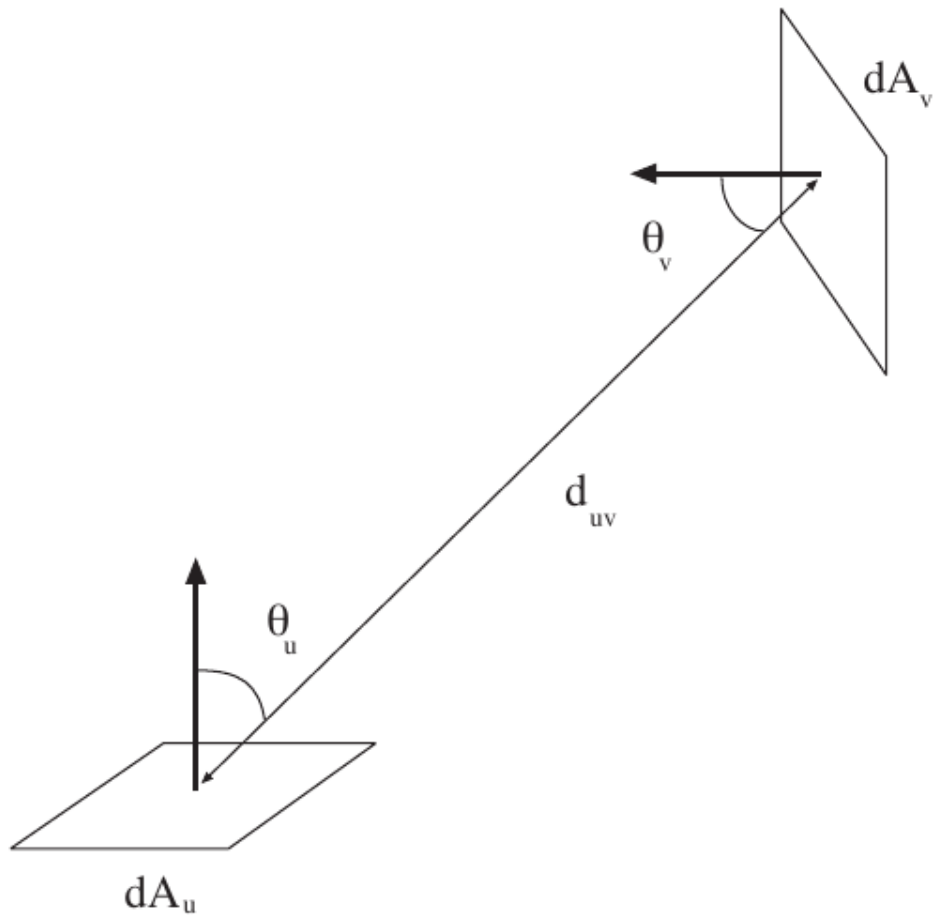


Figure 3.16. Terminology for expression derived in the text for the interreflection kernel.

计算出射度

1 2 3 4 5 6 7 8 9 10 11 12 13 14 15 16 17 18 19 20 21 22 23 24 25 26 27 28 29 30 31 32 33 34 35 36 37

$$B(\mathbf{u}) = E(\mathbf{u}) + B_{\text{incoming}}(\mathbf{u})$$

$$B_{\text{incoming}}(\mathbf{u}) = \rho_d(\mathbf{u}) \int_{\text{world}} \text{visible}(\mathbf{u}, \mathbf{v}) B(\mathbf{v}) \frac{\cos\theta_u \cos\theta_v}{\pi d_{uv}^2} dA_{\mathbf{v}}$$

$$= \rho_d(\mathbf{u}) \int_{\text{world}} \text{visible}(\mathbf{u}, \mathbf{v}) B(\mathbf{v}) K(\mathbf{u}, \mathbf{v}) dA_{\mathbf{v}}$$

$$B_{j \rightarrow i}(\mathbf{x}) = \rho_d(x) \int_{\text{patch } j} \text{visible}(\mathbf{x}, \mathbf{v}) K(\mathbf{x}, \mathbf{v}) dA_{\mathbf{v}} B_j$$

$$\bar{B}_{j \rightarrow i} = \frac{1}{A_i} \int_{\text{path } i} \rho_d(x) \int_{\text{patch } j} \text{visible}(\mathbf{x}, \mathbf{v}) K(\mathbf{x}, \mathbf{v}) dA_{\mathbf{v}} dA_{\mathbf{x}} B_j$$

1 2 3 4 5 6 7 8 9 10 11 12 13 14 15 16 17 18 19 20 21 22 23 24 25 26 27 28 29 30 31 32 33 34 35 36 37

$$\begin{aligned} B_i &= E_i + \sum_{\text{all } j} B_{\text{average incoming at } i \text{ from } j} \\ &= E_i + \sum_{\text{all } j} K_{ij} B_j \end{aligned}$$

where

$$K_{ij} = \frac{1}{A_i} \int_{\text{path } i} \rho_d(x) \int_{\text{patch } j} \text{visible}(\mathbf{x}, \mathbf{v}) K(\mathbf{x}, \mathbf{v}) dA_{\mathbf{v}} dA_{\mathbf{x}}$$